

# MBTPS2 Mutation Causes BRESEK/BRESHECK Syndrome

Misako Naiki,<sup>1,2</sup> Seiji Mizuno,<sup>3</sup> Kenichiro Yamada,<sup>1</sup> Yasukazu Yamada,<sup>1</sup> Reiko Kimura,<sup>1</sup> Makoto Oshiro,<sup>4</sup> Nobuhiko Okamoto,<sup>5</sup> Yoshio Makita,<sup>6</sup> Mariko Seishima,<sup>7</sup> and Nobuaki Wakamatsu<sup>1\*</sup>

<sup>1</sup>Department of Genetics, Institute for Developmental Research, Aichi Human Service Center, Kasugai, Aichi, Japan

<sup>2</sup>Department of Pediatrics, Nagoya University Graduate School of Medicine, Nagoya, Aichi, Japan

<sup>3</sup>Department of Pediatrics, Central Hospital, Aichi Human Service Center, Kasugai, Aichi, Japan

<sup>4</sup>Department of Pediatrics, Japanese Red Cross Nagoya Daiichi Hospital, Nagoya, Aichi, Japan

<sup>5</sup>Department of Medical Genetics, Osaka Medical Center and Research Institute for Maternal and Child Health, Izumi, Osaka, Japan

<sup>6</sup>Education Center, Asahikawa Medical University, Asahikawa, Hokkaido, Japan

<sup>7</sup>Department of Dermatology, Gifu University Graduate School of Medicine, Gifu, Gifu, Japan

Received 25 July 2011; Accepted 17 October 2011

BRESEK/BRESHECK syndrome is a multiple congenital malformation characterized by brain anomalies, intellectual disability, ectodermal dysplasia, skeletal deformities, ear or eye anomalies, and renal anomalies or small kidneys, with or without Hirschsprung disease and cleft palate or cryptorchidism. This syndrome has only been reported in three male patients. Here, we report on the fourth male patient presenting with brain anomaly, intellectual disability, growth retardation, ectodermal dysplasia, vertebral (skeletal) anomaly, Hirschsprung disease, low-set and large ears, cryptorchidism, and small kidneys. These manifestations fulfill the clinical diagnostic criteria of BRESHECK syndrome. Since all patients with BRESEK/BRESHECK syndrome are male, and X-linked syndrome of ichthyosis follicularis with atrichia and photophobia is sometimes associated with several features of BRESEK/BRESHECK syndrome such as intellectual disability, vertebral and renal anomalies, and Hirschsprung disease, we analyzed the causal gene of ichthyosis follicularis with atrichia and photophobia syndrome, *MBTPS2*, in the present patient and identified a p.Arg429His mutation. This mutation has been reported to cause the most severe type of ichthyosis follicularis with atrichia and photophobia syndrome, including neonatal and infantile death. These results demonstrate that the p.Arg429His mutation in *MBTPS2* causes BRESEK/BRESHECK syndrome. © 2011 Wiley Periodicals, Inc.

**Key words:** BRESEK/BRESHECK syndrome; IFAP syndrome; *MBTPS2*; mutation; S2P

## INTRODUCTION

BRESEK/BRESHECK syndrome (OMIM# 300404), a multiple congenital malformation disorder characterized by brain anomalies, intellectual disability, ectodermal dysplasia, skeletal deformities, Hirschsprung disease, ear or eye anomalies, cleft palate or

### How to Cite this Article:

Naiki M, Mizuno S, Yamada K, Yamada Y, Kimura R, Oshiro M, Okamoto N, Makita Y, Seishima M, Wakamatsu N. 2011. *MBTPS2* mutation causes BRESEK/BRESHECK syndrome.

Am J Med Genet Part A .

cryptorchidism, and kidney dysplasia/hypoplasia [Reish et al., 1997]. The acronym BRESEK refers to the common findings, whereas BRESHECK refers to all manifestations. Because the first two patients were maternally related half brothers, an X-linked disorder was proposed. Although each symptom of these patients is often observed in other congenital diseases, the combination of all symptoms is rare, and only one additional patient with BRESEK has been reported to date [Tumialán and Mapstone, 2006]. Here, we present the fourth male patient with multiple anomalies. The patient presented with a variety of clinical features that were consistent with those of the previously reported BRESHECK syndrome.

The syndrome of ichthyosis follicularis with atrichia and photophobia (IFAP, OMIM# 308205), an X-linked recessive oculocutaneous disorder, is characterized by a peculiar triad of ichthyosis follicularis, total or subtotal atrichia, and varying degrees

Grant sponsor: Takeda Science Foundation; Grant sponsor: Health Labour Sciences Research Grant.

\*Correspondence to:

Nobuaki Wakamatsu, Department of Genetics, Institute for Developmental Research, Aichi Human Service Center, 713-8 Kamiya-cho, Kasugai, Aichi 480-0392, Japan. E-mail: nwaka@inst-hsc.jp

Published online 00 Month 2011 in Wiley Online Library (wileyonlinelibrary.com).

DOI 10.1002/ajmg.a.34373

of photophobia [MacLeod, 1909]. Martino et al. [1992] reported a male patient with IFAP syndrome presented with short stature, intellectual disability, seizures, hypohidrosis, enamel dysplasia, congenital aganglionic megacolon, inguinal hernia, vertebral and renal anomalies, and the classic symptom triad of IFAP syndrome. This report broadened the clinical features of IFAP syndrome. It should be noted that the clinical symptoms of this patient are quite similar to those of BRESHECK syndrome, with the exception of cleft palate, cryptorchidism, and photophobia (Patient 5; Table I). The gene mutated in patients with IFAP syndrome, *MBTPS2* (GenBank reference sequence NM\_015884), was identified from a variety of clinical features of IFAP syndrome, including the triad and neonatal death [Oeffner et al., 2009]. Thus, the mode of inheritance and several clinical features are common to both BRESEK/BRESHECK and IFAP syndromes. These findings prompted us to perform mutation analysis of *MBTPS2* in the present patient, resulting in the identification of a missense mutation.

## MATERIALS AND METHODS

### Patients

Written informed consent was obtained from the parents of the patient. Experiments were conducted after approval of the institutional review board of the Institute for Developmental Research, Aichi Human Service Center. The patient (II-1; Fig. 3) was born to a 31-year-old mother (I-2) and a 31-year-old father (I-1), both healthy Japanese individuals without consanguinity. His mother miscarried her first child at 5 weeks. The pregnancy of the patient reported here was complicated with mild oligohydramnios, and he was delivered by caesarean because of a breech position at 38 weeks of gestation. His birth weight was 1,996 g (−2.6 SD), and he measured 44 cm (−2.6 SD) in length with an occipitofrontal circumference of 32.5 cm (−0.5 SD). Apgar scores at 1 and 5 min were four and eight, respectively. The patient exhibited generalized alopecia and lacked eyelashes, scalp hair, and eyebrows (Fig. 1A). The skin on the entire body was erythematous with

TABLE I. Clinical Features of BRESEK/BRESHECK and IFAP Syndromes and *MBTPS2* Mutation

Patient	BRESEK/BRESHECK syndrome				IFAP syndrome		
	1	2	3	4	5	6	7
Clinical features							
Gender	M	M	M	M	M	M	M
Gestational age (weeks)	32	40	ND	38	30	ND	ND
Birth weight (g)	990	2,230	ND	1,996	2,040	ND	ND
Intrauterine growth retardation	+	+	ND	+	−	ND	ND
Major features							
Follicular ichthyosis	−	−	ND	−	+	+	+
Atrichia	+	+	+	+	+	+	+
Photophobia	−	−	−	+	+	+	+
Brain malformation	+	+	+	+	+	−	+
Mental and growth retardation	+	+	+	+	+	+	+
Skeletal (Vertebrate) anomalies	+	+	+	+	+	+	+
Hirschsprung disease	−	+	+	+	+	+	+
Eye malformation or	+	+	+	−	+	−	−
Large ears	+	+	+	+	+	−	−
Cleft lip/palate or	−	+	−	−	−	+	−
Cryptorchidism	+	+	−	+	−	−	−
Kidney malformation	+	+	−	+	+	+	+
Other features							
Microcephaly	+	+	+	+	+	−	+
Seizures	−	+	+	+	+	−	+
Deafness	−	+	−	+	−	−	−
Hand anomalies	+	+	+	−	+	+	+
Cardiac anomalies	−	−	+	−	−	−	+
Inguinal hernia	−	−	−	−	+	+	+
Trachea anomalies	−	−	−	+	−	−	−
Regression	−	−	−	+	−	−	−
Age	6 h d	7 y	1.5 y	8 y	3 y	9 m d	14 m d
<i>MBTPS2</i> mutation	NP	NP	NP	R429H	NP	R429H	R429H

+, present; −, not present; M, male; ND, not described; NP, not performed; h, hour; d, day; m, month; y, year; R429H, Arg429His; BRESEK/BRESHECK syndrome, [Patients 1-4]; IFAP syndrome, [Patients 5-7]; Patients: 1, Reish et al. [1997] patient 1; 2, Reish et al. [1997] patient 2; 3, Tumialán and Mapstone [2006]; 4, present case; 5, Martino et al. [1992]; 6, Oeffner et al. [2009] 3-III:3; 7, Oeffner et al. [2009] 3-III:4.

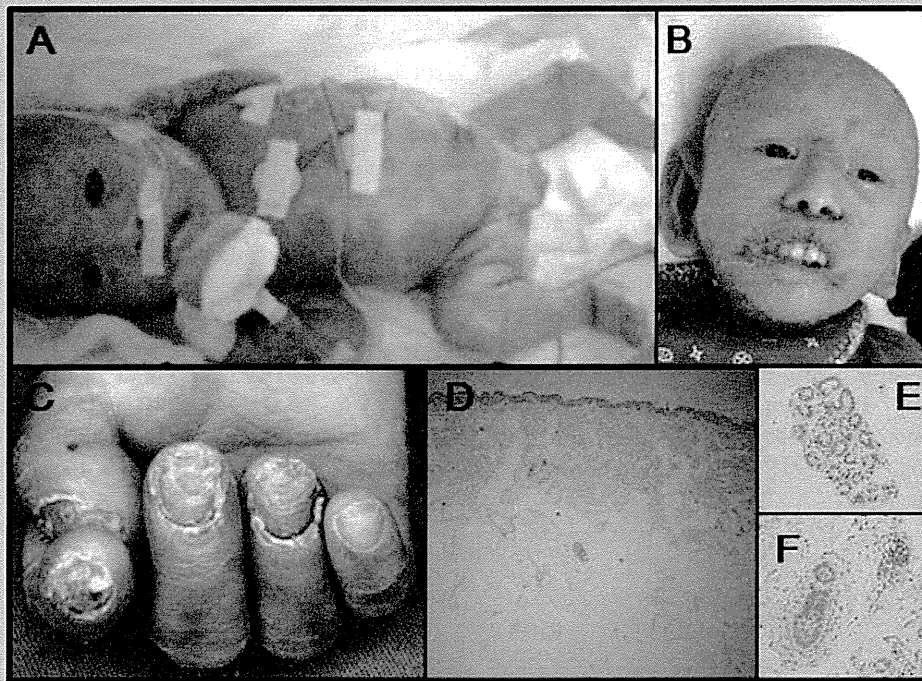


**FIG. 1.** Clinical appearance and dermatological findings of the patient. **A:** Lateral view of the patient at birth. Note the generalized alopecia with an absence of scalp hair, eyebrows, and eyelashes. The skin was dry and scaly, and an itchy erythema was observed over the entire body. **B:** Frontal view of the patient at 4 years of age. Note the characteristic facial appearance with long, malformed ears, a relatively high nasal bridge, and a wide nasal base. **C:** The patient had normal-sized but deformed and thickened nails. **D–F:** Histologic examination of the abdominal skin at the age of 15 months showed a reduced number of hair follicles (**D**), normal eccrine glands (**E**), and hypoplastic hair follicles (**F**).

continuous desquamation (Fig. 1A). He had malformed large ears, an inferiorly curved penis, and a bifid scrotum. The testicles were not palpable. He experienced persistent constipation, and total colonic Hirschsprung disease was confirmed through barium enema (Fig. 2E) and rectal biopsy at 2 months. A bone survey performed using three-dimensional (3D) computed tomography (CT) showed abnormal imbalanced hemivertebrae in the two lowest thoracic vertebral bodies (Fig. 2C). The patient's right kidney was smaller than normal. Brain magnetic resonance imaging (MRI) at 3 years of age demonstrated decreased volumes of the frontal and parietal lobes and thinning of the corpus callosum with dilatation of the ventricles (Fig. 2A,B). There were no abnormalities of the eyes or optic nerves. We concluded that the patient had BRESHECK syndrome. The patient had seizures at 5 months of age with an apneic episode and cyanosis. Electroencephalographic (EEG) analysis showed abnormal patterns of sharp waves in the posterior lobe. The seizures were almost completely controlled with phenobarbital. The patient was allergic to milk. At 7 months, tracheal endoscopy revealed subglottic tracheal stenosis and abnormal segmentation of the left lung. A chest CT performed at 3 years of age showed a congenital cystic adenomatoid malformation (CCAM) in the right upper lobe (Fig. 2D). Auditory brain stem responses showed bilateral 80 dB hearing loss at 8 months of age.

The patient exhibited delayed psychomotor development during his infancy. He could drink from a bottle at the age of 3 months and could sit up unsupported at 15 months. Abdominal skin biopsy at 15 months revealed reduced number of hair follicles (Fig. 1D). The eccrine glands were normal (Fig. 1E), and most of his hair follicles appeared to be hypoplastic (Fig. 1F). These findings were similar to ichthyosiform erythroderma. Photophobia was noted when the patient left the hospital and first went outside at 18 months of age. At 2 years and 6 months of age, he had a series of epileptic episodes. He experienced a maximum of 100 seizures per day, and EEG analysis showed continual abnormal spikes in the posterior lobe. The seizures were controlled with clonazepam therapy. At 2 years and 9 months of age, he could stand with support and displayed social smiles when interacting with other people. However, the patient developed psychomotor regression at the age of 3 years. He exhibited a progressive loss of emotional response to others, developed hypotonia, and could not stand or sit alone. At 4 years of age, he became bedridden and showed almost no response to people. He had highly desquamated skin, similar to that seen in ichthyosis (Fig. 1B), and easily developed erythema on the skin of the entire body. The patient had deformed and thickened nails (Fig. 1C). He had persistent corneal erosions, but ophthalmoscopy could not be performed at the age of 4 years because of corneal opacification.

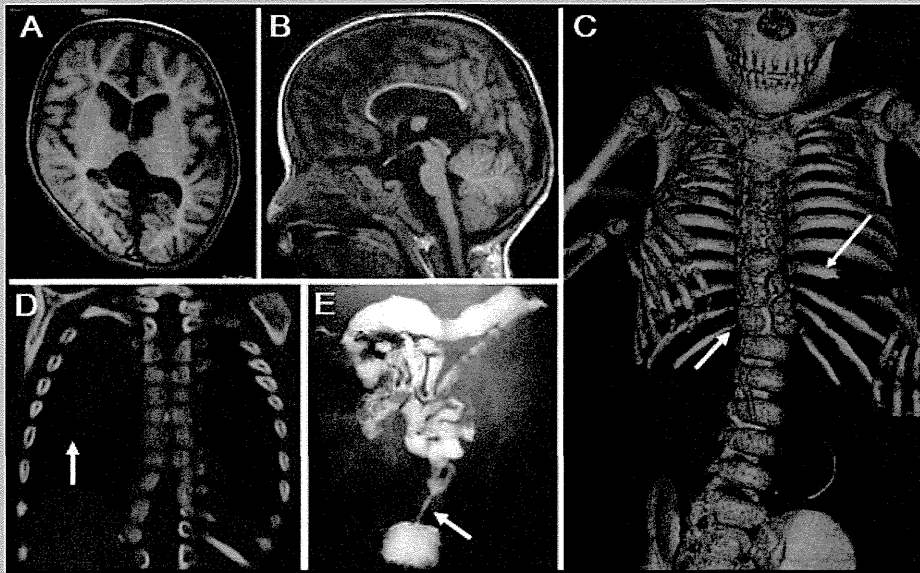


**FIG. 2.** CT and MRI findings of the patient. A,B: Brain MRI (T1-weighted image) at 3 years of age showed decreased volume of the cortex in the frontal and parietal lobes, the presence of a subdural cyst in the corpora quadrigemina, and dilatation of the lateral and fourth ventricle. C: A bone survey performed using 3D CT showed abnormal segmentation of the ninth rib and an imbalanced hemivertebrae in the two lowest thoracic vertebral bodies (shown with arrows). D: CT of the chest showed CCAM (indicated by the arrow) in the right upper lobe. E: Barium enema showed a reduced caliber rectum (indicated by the arrow), suggesting that the patient had Hirschsprung disease.

## Chromosomal and Molecular Genetic Studies

Genomic DNA isolated from the patient's peripheral white cells by phenol/chloroform extraction was used for *MBTPS2* mutation analysis. PCR-amplified DNA fragments were isolated using the QIAEX II Gel Extraction Kit (Qiagen, Valencia, CA) and purified using polyethylene glycol 6000 precipitation. PCR products were sequenced with the Big Dye Terminator Cycle Sequencing Kit V1.1 and analyzed with the ABI PRISM 310 Genetic Analyzer (Life Technologies, Carlsbad, CA). We also performed G-banded chromosome analysis at a resolution of 400–550 bands, genome-wide subtelomere fluorescence in situ hybridization (FISH) analysis, and array comparative genomic hybridization (array CGH) using Whole Human Genome Oligo Microarray Kits 244K (Agilent Technologies Inc., Palo Alto, CA) to identify genomic abnormalities.

## RESULTS

G-banded chromosome analysis and genome-wide subtelomere FISH analyses did not show chromosomal rearrangements in the patient. Array CGH analysis did not show copy number changes in the patient's genome with the exception of known copy-number variations (CNVs). Since some patients with IFAP syndrome have been reported to present with several clinical features of BRESEK/BRESHECK syndrome, including severe intellectual disability, vertebral and renal anomalies, and Hirschsprung disease, we conducted a comprehensive sequencing analysis of all exons and intron–exon boundaries of *MBTPS2*. This analysis identified a

missense mutation (c.1286G>A, [p.Arg429His]) in exon 10, which was previously reported for IFAP syndrome (Fig. 3). The mutation was also found in one allele of the mother (I-2), indicating that the mutation was of maternal origin and that the mother was a heterozygous carrier (Fig. 3).

## DISCUSSION

In this report, we describe the fourth male patient with BRESHECK syndrome in whom we identified a missense mutation (c.1286G>A, [p.Arg429His]) in *MBTPS2*, which is the causal gene for IFAP syndrome. *MBTPS2* encodes a membrane-embedded zinc metalloprotease, termed site-2 protease (S2P). S2P cleaves and activates cytosolic fragments of sterol regulatory element binding proteins (SREBP1 and SREBP2) and a family of bZIP membrane-bound transcription factors of endoplasmic reticulum (ER) stress sensors (ATF6, OASIS), after a first luminal proteolytic cut by site-1 protease (S1P) within Golgi membranes [Sakai et al., 1996; Ye et al., 2000; Kondo et al., 2005; Asada et al., 2011]. The SREBPs control the expression of many genes involved in the biosynthesis and uptake of cholesterol, whereas ATF6 and OASIS induce many genes that clean up accumulated unfolded proteins in the ER. Dysregulated SREBP activation, impaired lipid metabolism, and accumulation of unfolded proteins in the ER caused by *MBTPS2* mutations could lead to disturbed differentiation of epidermal structures, resulting in the symptom triad of IFAP syndrome [Cursiefen et al., 1999; Traboulsi et al., 2004; Elias et al., 2008]. Oeffner et al. [2009] first identified five missense mutations in *MBTPS2* in patients with IFAP

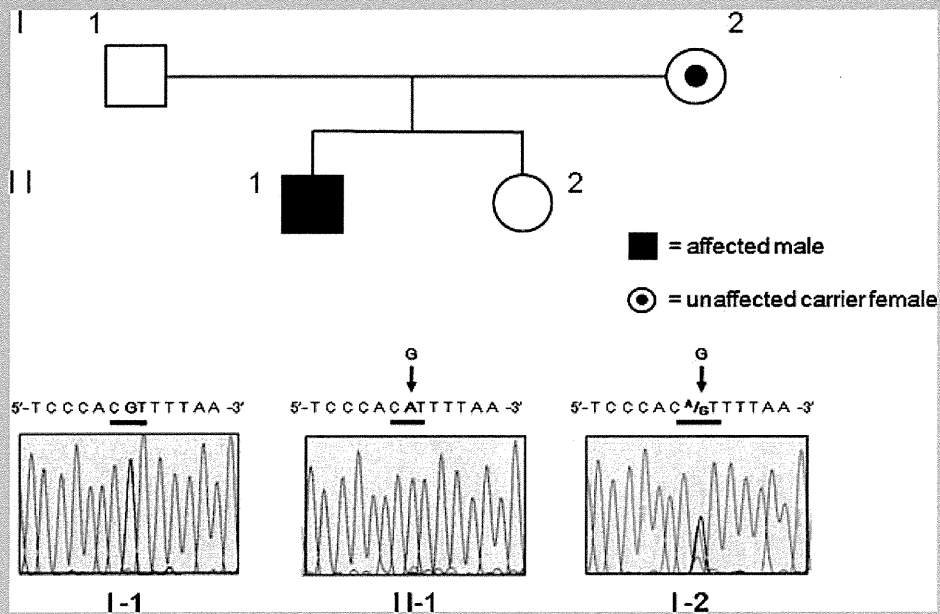


FIG. 3. Identification of a disease mutation. The sequence analyses of the patient (II-1) showed a c.1286G>A variant in exon 10 of *MBTPS2*, which predicts p.Arg429His, as indicated by the arrow (middle panel). The mother (I-2) was heterozygous for the mutation (C<sup>A/G</sup>T) (right panel).

syndrome. Transfection studies using wild type and mutant *MBTPS2* expression constructs demonstrated that the five *MBTPS2* mutations did not affect S2P protein amount and localization in the ER. However, enzyme activities, as measured by sterol responsiveness, were decreased in S2P-deficient M19 cells when the mutant *MBTPS2* was transiently expressed. Interfamilial phenotypic differences between male IFAP patients and the properties of mutants in functional assays predict a genotype–phenotype correlation, ranging from mild forms of the triad with relatively high enzyme activity (~80%) to severe manifestations of intellectual disability, various developmental defects, and early death with low enzyme activity (~15%). The identified p.Arg429His mutation in the patient reported here is one of the five missense mutations with the lowest enzyme activity. It was previously reported that all four patients harboring the p.Arg429His mutation died within 14 months of birth. The five mutations were not located in the HEIGH motif (amino acids [aa] 171–175) or in the LD<sub>467</sub>G sequence, both of which are regions important for coordinating the zinc atom at the enzymatic active site for protease activity in the Golgi membrane [Zelenski et al., 1999]. However, among the five mutations, the p.Arg429His mutation is located closest to the intramembranous domain, and it strongly reduced the enzymatic activity and caused a severe phenotype. This finding suggests that mutations in the HEIGH motif or in the LD<sub>467</sub>G sequence are fatal because they lead to a null function of the S2P. Although the detailed skin findings of the four patients with the p.Arg429His mutation have not been reported, it should be noted that one of the four patients (3-III:4) with the p.Arg429His mutation had brain anomaly, seizures, psychomotor retardation, vertebrae anomaly, Hirschsprung disease, absence of a kidney, atrial septum defect, and inguinal

hernia, in addition to the symptom triad of IFAP syndrome [Oeffner et al., 2009]. These symptoms overlap with the majority of symptoms observed in BRESHECK syndrome (BRESCHK; six of eight symptoms observed in BRESHECK) (Table I), and the present patient has BRESHECK syndrome. Collectively, these observations suggest that the most severe form of the syndrome caused by the p.Arg429His mutation in *MBTPS2* shows features quite similar or identical to those of BRESEK/BRESHECK syndrome.

There are two major differences in the definitions of IFAP syndrome and BRESEK/BRESHECK syndrome. Ichthyosis follicularis, one of the triad symptoms of IFAP syndrome, is a clinical condition of the skin. However, several studies on IFAP syndrome have reported various skin eruptions such as psoriasis-like and ichthyosis-like eruptions [Martino et al., 1992; Sato-Matsumura et al., 2000]. In contrast, patients with BRESEK/BRESHECK syndrome showed severe lamellar desquamation with diffuse scaling [Reish et al., 1997], similar to that observed in the present patient. This could be because of the difference in features of the skin, namely, ichthyosiform erythroderma-like appearance versus ichthyosis follicularis, in patients with the most severe forms of *MBTPS2* mutation and patients with IFAP syndrome who were described earlier, respectively.

The second difference is that photophobia was not described in the reported three male patients with BRESEK/BRESHECK syndrome [Reish et al., 1997; Tumialán and Mapstone, 2006]. In the present patient, photophobia became evident after he was diagnosed with BRESHECK syndrome. Photophobia is a symptom of epithelial disturbances of the cornea, such as ulceration and vascularization, which result in corneal scarring [Traboulsi et al., 2004]. In the most severe cases of *MBTPS2* mutation, such as

patients with severe intellectual disability who are bedridden and die early, it is likely that the patients were treated in the hospital without being exposed to sunlight. Therefore, it would be difficult to observe photophobia as a main symptom in those cases. Moreover, two previously described patients with BRESEK/BRESHECK syndrome had initial maldevelopment of one eye or small optic nerves. In these patients, photophobia may not have been obvious because of malformations of the eyes and optic nerves [Reish et al., 1997]. In our study, the patient showed clinical features of BRESHECK syndrome and photophobia with *MBTPS2* mutation, indicating that the clinical features of the present patient are extremely broad compared to the features of IFAP syndrome caused by *MBTPS2* mutation that have been previously reported [MacLeod, 1909].

Recently, a missense mutation (c.1523A>G, [p.Asn508Ser]) in *MBTPS2* was identified from 26 cases of three independent families with keratosis follicularis spinulosa decalvans (KFSD; OMIM# 308800), which is characterized by the development of hyperkeratotic follicular papules on the scalp followed by progressive alopecia of the scalp, eyelashes, and eyebrows in addition to childhood photophobia and corneal dystrophy [Aten et al., 2010]. A significant association was found between KFSD and the p.Asn508Ser mutation. The specific localization of alopecia to the scalp, eyelashes, and eyebrows and the limited childhood photophobia of KFSD indicate that KFSD has a relatively mild phenotype. The authors postulate that IFAP syndrome and KFSD are within the spectrum of one genetic disorder with a partially overlapping phenotype and propose that a new name should be chosen for KFSD/IFAP syndrome with an *MBTPS2* mutation. In contrast, the BRESHECK syndrome observed in the present patient has a severe phenotype caused by the p.Arg429His mutation. The present patient and the two patients (3-III:3 and 3-III:4) with the p.Arg429His mutation displayed broader clinical features, including eight features (BRESHECK) and six features (RESHCK and BRESHK) of BRESEK/BRESHECK syndrome, respectively (patients 4, 6, and 7; Table I) [Oeffner et al., 2009]. There is a debate regarding whether the two patients harboring six features were correctly diagnosed with BRESEK/BRESHECK syndrome since the patients did not have “BRESEK” but rather a combination of six other clinical features. To better understand and clearly distinguish the clinical features of the present patient from those of the reported patients with *MBTPS2* mutations, we propose the nomenclature of “BRESHECK/IFAP syndrome” for the present patient because he has clinical features of BRESHECK syndrome. We also suggest that the BRESHECK/IFAP syndrome be used for a broader definition that would include patients harboring most features of BRESHECK syndrome, including the previously reported two patients (3-III:3 and 3-III:4) with p.Arg429His mutation in *MBTPS2* [Oeffner et al., 2009]. Data from further genetic and clinical studies on more patients are required to determine which genes or *MBTPS2* mutations are associated with BRESEK/BRESHECK or BRESHECK/IFAP syndrome, respectively.

## ACKNOWLEDGMENTS

We thank the patient and his family for participating in the study. This study was supported by the Takeda Science Foundation

(to N.W.) and by the Health Labour Sciences Research Grant (to S.M. and N.W.).

## REFERENCES

- Aten E, Brasz LC, Bornholdt D, Hooijkaas IB, Porteous ME, Sybert VP, Vermeer MH, Vossen RH, van der Wielen MJ, Bakker E, Breuning MH, Grzeschik KH, Oosterwijk JC, den Dunnen JT. 2010. Keratosis follicularis spinulosa decalvans is caused by mutations in *MBTPS2*. *Hum Mutat* 31:1125–1133.
- Asada R, Kanemoto S, Kondo S, Saito A, Imaizumi K. 2011. The signalling from endoplasmic reticulum-resident bZIP transcription factors involved in diverse cellular physiology. *J Biochem* 149:507–518.
- Cursiefen C, Schlötzer-Schrehardt U, Holbach LM, Pfeiffer RA, Naumann GOH. 1999. Ocular findings in ichthyosis follicularis, atrichia, and photophobia syndrome. *Arch Ophthalmol* 117:681–684.
- Elias PM, Williams ML, Holleran WM, Jiang YJ, Schmuth M. 2008. Pathogenesis of permeability barrier abnormalities in the ichthyoses: Inherited disorders of lipid metabolism. *J Lipid Res* 49:697–714.
- Kondo S, Murakami T, Tatsumi K, Ogata M, Kanemoto S, Otori K, Iseki K, Wanaka A, Imaizumi K. 2005. OASIS, a CREB/ATF-family member, modulates UPR signalling in astrocytes. *Nat Cell Biol* 7:186–194.
- MacLeod JMH. 1909. Three cases of ‘ichthyosis follicularis’ associated with baldness. *Br J Dermatol* 21:165–189.
- Martino F, D’Eufemia P, Pergola MS, Finocchiaro R, Celli M, Giampà G, Frontali M, Giardini O. 1992. Child with manifestations of dermatichic syndrome and ichthyosis follicularis alopecia photophobia (IFAP) syndrome. *Am J Med Genet* 44:233–236.
- Oeffner F, Fischer G, Happle R, König A, Betz RC, Bornholdt D, Neidel U, Boente Mdel C, Redler S, Romero-Gomez J, Salhi A, Vera-Casaño A, Weirich C, Grzeschik KH. 2009. IFAP syndrome is caused by deficiency in *MBTPS2*, an intramembrane zinc metalloprotease essential for cholesterol homeostasis and ER stress response. *Am J Hum Genet* 84:459–467.
- Reish O, Gorlin RJ, Hordinsky M, Rest EB, Burke B, Berry SA. 1997. Brain anomalies, retardation of mentality and growth, ectodermal dysplasia, skeletal malformations, Hirschsprung disease, ear deformity and deafness, eye hypoplasia, cleft palate, cryptorchidism, and kidney dysplasia/hypoplasia (BRESEK/BRESHECK): New X-linked syndrome? *Am J Med Genet* 68:386–390.
- Sakai J, Duncan EA, Rawson RB, Hua X, Brown MS, Goldstein JL. 1996. Sterol-regulated release of SREBP-2 from cell membranes requires two sequential cleavages, one within a transmembrane segment. *Cell* 85:1037–1046.
- Sato-Matsumura KC, Matsumura T, Kumakiri M, Hosokawa K, Nakamura H, Kobayashi H, Ohkawara A. 2000. Ichthyosis follicularis with alopecia and photophobia in a mother and daughter. *Br J Dermatol* 142:157–162.
- Traboulsi E, Waked N, Mégarbané H, Mégarbané A. 2004. Ocular findings in ichthyosis follicularis–alopecia–photophobia (IFAP) syndrome. *Ophthalmol* 25:153–156.
- Tumialán LM, Mapstone TB. 2006. A rare cause of benign ventriculomegaly with associated syringomyelia: BRESEK/BRESHECK syndrome. Case illustration. *J Neurosurg* 105:155.
- Ye J, Rawson RB, Komuro R, Chen X, Davé UP, Prywes R, Brown MS, Goldstein JL. 2000. ER stress induces cleavage of membrane-bound ATF6 by the same proteases that process SREBPs. *Mol Cell* 6:1355–1364.
- Zelenski NG, Rawson RB, Brown MS, Goldstein JL. 1999. Membrane topology of S2P, a protein required for intramembraneous cleavage of sterol regulatory element-binding proteins. *J Biol Chem* 274:21973–21980.

## ORIGINAL ARTICLE

# Reduced *PLP1* expression in induced pluripotent stem cells derived from a Pelizaeus–Merzbacher disease patient with a partial *PLP1* duplication

Keiko Shimojima<sup>1,2</sup>, Takahito Inoue<sup>3</sup>, Yuki Imai<sup>4</sup>, Yasuhiro Arai<sup>5</sup>, Yuta Komoike<sup>6</sup>, Midori Sugawara<sup>2</sup>, Takako Fujita<sup>3</sup>, Hiroshi Ideguchi<sup>3</sup>, Sawa Yasumoto<sup>3</sup>, Hitoshi Kanno<sup>7</sup>, Shinichi Hirose<sup>3</sup> and Toshiyuki Yamamoto<sup>2</sup>

Pelizaeus–Merzbacher disease (PMD) is an X-linked recessive disorder characterized by dysmyelination of the central nervous system (CNS). We identified a rare partial duplication of the proteolipid protein 1 gene (*PLP1*) in a patient with PMD. To assess the underlying effect of this duplication, we examined *PLP1* expression in induced pluripotent stem (iPS) cells generated from the patient's fibroblasts. Disease-specific iPS cells were generated from skin fibroblasts obtained from the indicated PMD patient and two other PMD patients having a 637-kb chromosomal duplication including entire *PLP1* and a novel missense mutation (W212C) of *PLP1*, by transfections of *OCT3/4*, *C-MYC*, *KLF4* and *SOX2* using retro-virus vectors. *PLP1* expressions in the generated iPS cells were examined by northern blot analysis. Although *PLP1* expression was confirmed in iPS cells generated from two patients with the entire *PLP1* duplication and the missense mutation of *PLP1*, iPS cells generated from the patient with the partial *PLP1* duplication manifesting a milder form of PMD showed null expression. This indicated that the underlying effect of the partial *PLP1* duplication identified in this study was different from other *PLP1* alterations including a typical duplication and a missense mutation.

*Journal of Human Genetics* (2012) 57, 580–586; doi:10.1038/jhg.2012.71; published online 14 June 2012

**Keywords:** Pelizaeus–Merzbacher disease (PMD); proteolipid protein 1 gene (*PLP1*); induced pluripotent stem (iPS) cells; partial duplication; dysmyelination

## INTRODUCTION

Pelizaeus–Merzbacher disease (PMD; MIM #312080) is an X-linked recessive neurodegenerative disorder characterized by dysmyelination of the central nervous system (CNS). Patients with PMD often present with nystagmus as the initial symptom, and psychomotor developmental delay associated with spasticity and ataxia is seen later in development.<sup>1–3</sup> The proteolipid protein 1 gene (*PLP1*; MIM #300401), located on chromosome Xq22.2, is the gene responsible for PMD. It encodes 2 isoforms, PLP1 and DM20, as a consequence of differential splicing of exon 3. The genetic basis of PMD is unique because two-thirds of *PLP1* abnormalities identified in PMD patients are duplications of small chromosomal segments that include *PLP1*. The remaining one-third of *PLP1* abnormalities are nucleotide alterations in the *PLP1* coding sequence. The nucleotide alterations in *PLP1* are varied and are scattered along the entire coding region of *PLP1*.<sup>1–3</sup>

Because *PLP1* is mainly expressed in oligodendrocytes in the CNS and cultured skin fibroblasts express low levels of *PLP1*, gene

expression in the fibroblasts has been analyzed by comparative reverse-transcription (RT)-PCR analysis.<sup>4,5</sup> The use of technology to establish induced pluripotent stem (iPS) cells has now made it possible to examine gene expression and function in greater detail.<sup>6</sup> In 2007, Takahashi *et al.* established iPS cells from human skin fibroblasts.<sup>7</sup> This revolutionary technology has stimulated and accelerated research in embryogenesis and genetics. In this study, we established iPS cells from skin fibroblasts of patients with PMD and examined *PLP1* expression. This is the first report analyzing *PLP1* expression in PMD disease-carrying iPS cells.

## MATERIALS AND METHODS

### Subjects

For our ongoing study identifying genomic mutations in *PLP1*, three new patients with dysmyelination were referred to us for genetic diagnosis based on the clinical diagnosis of PMD.<sup>8</sup> Clinical information and radiographic findings by MRI for the patients were obtained from attending doctors. Based on

<sup>1</sup>Precursory Research for Embryonic Science and Technology (PRESTO), Japan Science and Technology Agency (JST), Kawaguchi, Japan; <sup>2</sup>Tokyo Women's Medical University Institute for Integrated Medical Sciences, Tokyo, Japan; <sup>3</sup>Department of Pediatrics, School of Medicine, Fukuoka University, Fukuoka, Japan; <sup>4</sup>Department of Pediatrics and Child Health, Nihon University School of Medicine, Tokyo, Japan; <sup>5</sup>Tokyo Metropolitan Tobu Medical Center for Persons with Developmental/Multiple Disabilities, Tokyo, Japan; <sup>6</sup>Department of Hygiene and Public Health, Tokyo Women's Medical University, Tokyo, Japan and <sup>7</sup>Department of Transfusion Medicine and Cell Processing, Tokyo Women's Medical University, Tokyo, Japan

Correspondence: Dr T Yamamoto, Institute for Integrated Medical Sciences, Tokyo Women's Medical University, Kawada-cho 8-1, Shinjuku-ward, Tokyo 162-8666, Japan.

E-mail: yamamoto.toshiyuki@twmu.ac.jp

Received 19 March 2012; revised 15 May 2012; accepted 16 May 2012; published online 14 June 2012

approval by the ethical committees at the institutions, written informed consent was obtained from each patient and/or their family. Peripheral blood samples were collected from the patients and genotyping was performed as described.<sup>8</sup> After genetic diagnosis of PMD was made, another written informed consent for the iPS cell study was obtained from each patient and/or their family. Skin fibroblasts were collected from three patients and a healthy male control.

### Genotyping of the patients

Genomic DNAs were extracted from peripheral blood samples from patients and others by using standard methods. Initial screening for *PLP1* duplication was performed by multiplex ligation-dependent probe amplification analysis by using the PLP1 Kit (P022; MRC-Holland, Amsterdam, The Netherlands) according to the manufacturer's instruction.<sup>9</sup> In case of *PLP1* duplication, the aberration region was confirmed by microarray-based comparative genomic hybridization (aCGH) using the Agilent Human 105A CGH Kit (Agilent Technologies, Santa Clara, CA, USA) as described previously.<sup>8</sup> To detect the small duplication in Patient 1, a custom array was designed using e-array, a web-based software (<https://earray.chem.agilent.com/earray/>), and 29 918 probes in chrX:98 000 000–104 500 000, around *PLP1*, were selected. The average interval of the probes was 217 bp in this region.

*PLP1* duplication was confirmed by two-color fluorescence *in-situ* hybridization as described previously.<sup>8</sup> Two bacterial artificial chromosome clones, RP11–75D20 (located at Xp22.13) and RP11–832L2 (located at Xq22.2), were selected from the UCSC Human Genome Browser (<http://genome.ucsc.edu/>) and used as probes. The fixed metaphase and interphase spreads of the specimens were derived from patients' peripheral blood samples and generated iPS cells. The direction of the duplicated segment identified in Patient 2 was analyzed by fiber-fluorescence *in-situ* hybridization analysis as described previously.<sup>8</sup>

PCR and direct sequencing of all seven exons of *PLP1* was performed by standard methods using the primers reported by Hobson *et al.*<sup>4</sup> The designs of the primers for all exons and the breakpoint searches of the duplicated segments in Patient 1 are listed in Supplementary Table 1.

### Cell culture

Human fibroblasts, the Plat-E Retroviral Packaging Cell Line (Cell Biolabs, San Diego, CA, USA), 293FT cells (Life Technologies, Foster City, CA, USA) and mouse fibroblast STO cell line (SNL) feeder cells (ECACC, Salisbury, UK) were grown in Dulbecco's modified Eagle's medium (DMEM 14247-15; Nacalai Tesque, Japan) containing 10% fetal bovine serum and 0.5% penicillin and streptomycin (Life Technologies). Human iPS cells were maintained on SNL feeder cells treated with mitomycin C in Primate ES Cell Culture Medium supplemented with 4 ng ml<sup>-1</sup> recombinant basic fibroblast growth factor (# RCHMD001; Repro CELL, Yokohama, Japan) and passaged as described previously.<sup>7,10</sup>

### Generation of iPS cells

Disease-specific iPS cells were generated from patients' skin fibroblasts as previously described.<sup>7</sup> Briefly, recombinant lentivirus produced from 293FT cells, in which pLenti6/Ubc/mSlc7a1 (AddGene, Cambridge, MA, USA) was transfected by use of Virapower Lentiviral Expression System (Life Technologies), was infected into cultured fibroblasts for 24 h. Then, four retroviruses produced with Plat-E Packaging Cells (Cell Biolabs), in which pMXs-hOCT3/4, pMXs-hSOX2, pMXs-hKLF4 and pMXs-hc-MYC (AddGene) were transferred independently, were infected into mSlc7a1-expressing human fibroblasts. Six days after retroviral infection, the fibroblasts were placed onto mouse fibroblast SNL feeder cells (ECACC, Salisbury, UK) at the appropriate concentration. The following day, DMEM 14247-15 (Nacalai Tesque, Japan) was replaced with Primate ES Cell Culture Medium supplemented with 4 ng ml<sup>-1</sup> recombinant basic fibroblast growth factor (# RCHMD001; Repro CELL, Yokohama, Japan). Thirty days after transduction, each embryonic stem (ES) cell-like colony was individually placed onto SNL feeder cells. Each colony was tested to determine whether they had indeed acquired pluripotency. After validation,<sup>10</sup> three independent iPS cell clones were selected from the candidates generated from each patient's skin fibroblasts.

### Validation of the pluripotency of iPS cells

Initially, alkaline phosphatase staining was performed for validation of iPS cells. Leukocyte Alkaline Phosphatase (AP) kit 86R (Sigma-Aldrich, St Louis, MO, USA) was used for this purpose.

Reactivation of endogenous pluripotency genes and the silencing of artificially induced retroviral transgenes indicated successful reprogramming of putative iPS cell clones. To confirm this, RT-PCR analysis and real-time PCR were performed as described below.

Total RNAs were extracted from iPS cells using ISOGEN (Nippon Gene, Tokyo, Japan) and contaminating genomic DNAs were removed by DNase (Takara, Ohtsu, Japan) according to the manufacturer's instructions. Subsequently, total RNAs were reverse transcribed into complementary DNAs by using the Superscript VILO cDNA Synthesis Kit (Life Technologies) according to the manufacturer's instructions.

Quantitative real-time PCR was performed for *OCT3/4*, *SOX2*, *KLF4*, *C-MYC*, *NANOG*, *REX1*, *GAPDH* and actin beta using the Power SYBR Green PCR Master Mix (Life Technologies) and analyzed with the 7300 Real-Time PCR System (Life Technologies). Primer sequences are shown in Supplementary Table 1.

Immunocytochemistry was also performed for all putative iPS cells. For this purpose, the following primary antibodies were used: anti-SSEA4 (1:200, MAB1435, R&D systems, Minneapolis, MN, USA), anti-OCT3/4 (1:200, AF1759, R&D systems), anti-TRA-1-60 (1:200, MAB4360, Millipore, Billerica, MA, USA), and Anti-TRA-1-81 (1:200, MAB4381, Millipore). Secondary antibodies included Alexa488-conjugated donkey anti-mouse IgG, Alexa488-conjugated goat anti-mouse IgM, and Alexa594-conjugated donkey anti-mouse IgG (1:1000, Life Technologies). Nuclei were stained with Hoechst 33342 (1:1000, Life Technologies).

### Validation of the differentiation ability of iPS cells

Determination of the differentiation ability of established iPS cells is important for the selection of putative iPS cell clones. To confirm their pluripotency to differentiate into three embryonic germ layers, we used floating cultivation to form embryoid bodies as described previously.<sup>10</sup> iPS cells were grown as floating cultures for 8 days. After embryoid body formation, the cells were cultured on gelatin-coated dishes for an additional 8 days.

Immunocytochemistry was performed to confirm expression of the three germ layers as described elsewhere.<sup>10</sup> In this case, three primary antibodies were used; anti-βIII tubulin (1:1000, MRB435P, Covance, Princeton, NJ, USA) as the ectoderm marker, anti-α smooth muscle actin (1:200, A2547, Sigma-Aldrich) for mesoderm, and anti-αAFP (1:100, A8452, Sigma-Aldrich) for endoderm. Donkey anti-mouse IgG labeled with Alexa Fluor 594 and donkey anti-rabbit IgG labeled with Alexa Fluor 488 (1:1000, Life Technologies) were used as secondary antibodies. Nuclei were stained with Hoechst 33342 (1:1000, Life Technologies) for nuclear staining.

### Validation of the karyotypes of iPS cells

To check the artificial chromosomal rearrangements, conventional G-banding by trypsin treatment stained with Giemsa and aCGH analyses using the same methods described above were performed for the generated iPS cell clones. iPS cell lines that acquired chromosomal rearrangements were eliminated from this study.

### Database analysis

Preliminary gene expression analysis was performed using online data sets. Two microarray data sets, GSM242095 for adult human dermal fibroblasts and GSM241846 for iPS cells (clone 201B7),<sup>7</sup> were retrieved from NCBI Gene Expression Omnibus (GEO) and analyzed using GeneSpring GX10 (Agilent Technologies).

### Northern blotting

The full-length mRNA of *PLP1* (920 bp) and a partial sequence of actin beta (*ACTNB*; MIM #102630) mRNA (91 bp) were amplified by RT-PCR by using Human Brain Total RNA (#636530, Clontech, Mountain View, CA, USA) as a template. Primer sequences are listed in Supplementary Table 1. The PCR product was subcloned into pGEM-T Vector System (Promega, Madison, WI,

USA) and grown in LB Broth overnight. Plasmid DNAs were extracted by an automated DNA isolation system, PI-80X (Kurabo, Osaka, Japan). DNA inserts were digested with *SacI* and *SacII* restriction enzymes. Following agarose gel electrophoresis, product bands were excised and extracted using the QIAquick Gel Extraction Kit (QIAGEN, Hilden, Germany). The DNA fragments were then labeled using [ $\alpha$ - $^{32}$ P] dCTP (PerkinElmer, Waltham, MA, USA) and used as probes for northern blotting.

Hybridization was performed as described previously.<sup>11</sup> Briefly, 30  $\mu$ g of total RNA was extracted using ISOGEN (Nippon Gene, Tokyo, Japan) according to the manufacturer's instructions, separated on a 1% agarose/0.6M formaldehyde gel, visualized using Radiant Red RNA Stain (Bio-Rad, Hercules, CA, USA), transferred to a nylon membrane and subsequently hybridized for 24 h with either *PLP1* or *ACTNB* probes. Images were captured using the FLA-5100 scanner (Fujifilm, Tokyo, Japan).

Initial analysis included seven samples: mitomycin-treated and -untreated SNL feeder cells, Epstein-Barr virus-infected immortalized lymphocytes derived from a normal human control, human skin fibroblasts derived from the normal control, iPS cells generated from the normal human control and two brain samples purchased from a provider (Human Fetal Brain Total RNA #636526 and Human Brain Total RNA #636530, Clontech). Subsequent analysis included the 12 iPS cell lines generated in this study.

## RESULTS

### Clinical features

Patient 1 was a 16-year-old male, born by spontaneous delivery at 40 weeks gestation, with a weight of 3054 g. Soon after birth he showed nystagmus. At 4 months, he exhibited poor neck control and was diagnosed with spastic paraplegia. Psychomotor development was moderately delayed with walking alone at his age of 2 years and his intelligence quotient was estimated below 50. At 15 years, he was prescribed medication for depression. At that time, his fine motor ability allowed the use of chopsticks but he needed a wheel chair to move. His speech was dysarthric. One month later, he had an epileptic attack and was admitted to the hospital. An electroencephalogram revealed occipital spikes. Although auditory brain response was normal, brain magnetic resonance imaging (MRI) revealed a pattern of mild dysmyelination (Figures 1a and b).

Patient 2 was a 46-year-old male with two healthy female siblings. As he lacked neck control at 1 year of age, he was diagnosed with spastic cerebral palsy. Then, at 4 years, he could turn over but could not sit unaided. He lacked the ability to speak effectively, being limited to two-word sentences. At 15 years, he could use a wheel chair by himself. Subsequently, the quality of his daily life declined gradually. At 39 years, MRI revealed atrophic white matter displaying dysmyelination (Figure 1c). At present, he can move only his upper body very slowly and is bedridden. He is able to comprehend what his siblings say, but he is severely dysarthric and is able to speak only a few words very slowly.

Patient 3 was a 32-month-old boy with a birth weight of 3869 g delivered at 39 weeks gestation. He has a healthy brother. Owing to respiratory problems since birth, he was intubated and tracheostomy was performed at 58 days. He also required tube feeding. He is currently bedridden and has continuous nystagmus. Auditory-brain-response audiometry showed no waves after the first wave. A brain MRI revealed high-intensity lesions of the white matter in a T2-weighted image, indicating severe hypomyelination (Figure 1d).

### Molecular analyses

Initial multiplex ligation-dependent probe amplification analysis using a *PLP1* Kit (P022; MRC-Holland) identified duplications of *PLP1* in Patient 1 and 2 (data not shown).<sup>9</sup> Patient 2 had a duplication of all 7 exons of *PLP1*, and subsequent aCGH analysis

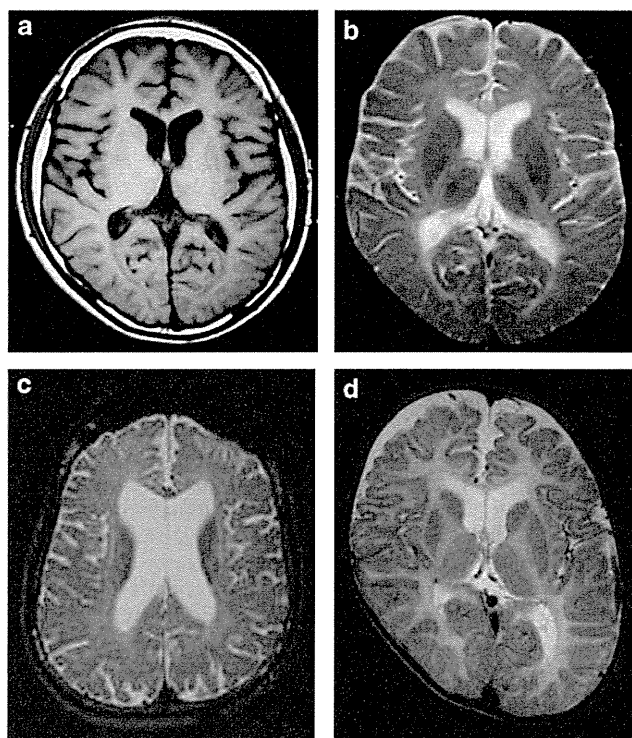


**Figure 1** Brain MRI findings of the patients T1- (a) and T2 (b) weighted images of Patient 1 show mild and diffuse volume loss of the brain and high-intensity signals of the deep white matter in T2 indicating mild dysmyelination. T2-weighted image of Patient 2 (c) shows diffuse volume loss resulting in the dilatation of the ventricles and dysmyelination in the white matter. T2-weighted image of Patient 3 (d) shows extremely hypomyelinated pattern with high intensity in all white matter.

by using the Human Genome CGH Microarray 105 K (Agilent Technologies) revealed that the duplicated region was chrX:102 519 000–103 155 851 (636 851 bp) with an average  $\log_2$  ratio of +0.83, which is a typical duplication region seen in PMD patients with *PLP1* duplications (Figure 2a). The duplication was confirmed by fluorescence *in-situ* hybridization (Figure 2b), and the direction of the duplicated segment, including *PLP1*, was shown to be in a tandem configuration by fiber-fluorescence *in-situ* hybridization analysis (Figure 2c).

The duplication identified in Patient 1 was unique because only the first 3 exons (exons 1–3) of *PLP1* were included in the duplicated region. To confirm this partial duplication, we designed a custom aCGH chip and used it to detect the precise duplication region. As shown in Figure 3a, the duplicated region was chrX:102 912 361–102 928 360 (15 999 bp) with an average  $\log_2$  ratio of +0.72. To determine the location of the duplicated segment, we sought to detect the breakpoint by PCR direct sequencing, using primers A and B (Supplementary Table 1). A 775-bp band was obtained and re-sequenced (Figures 3b and c). Ultimately, an extremely small duplication of 16 208 bp, which has never been previously reported, was identified. The sample from Patient 1's mother was also analyzed and she was found to be a carrier of this duplication (Figures 3b and c).

In Patient 3, a novel missense mutation, c.636G>C (W212C), was identified in exon 5 of *PLP1* (Figure 2d). The *PLP1* sequence is completely conserved among species and this novel mutation was not identified in 100 normal control samples (50 males and 50 females). This patient's mother declined to have her genotype analyzed.

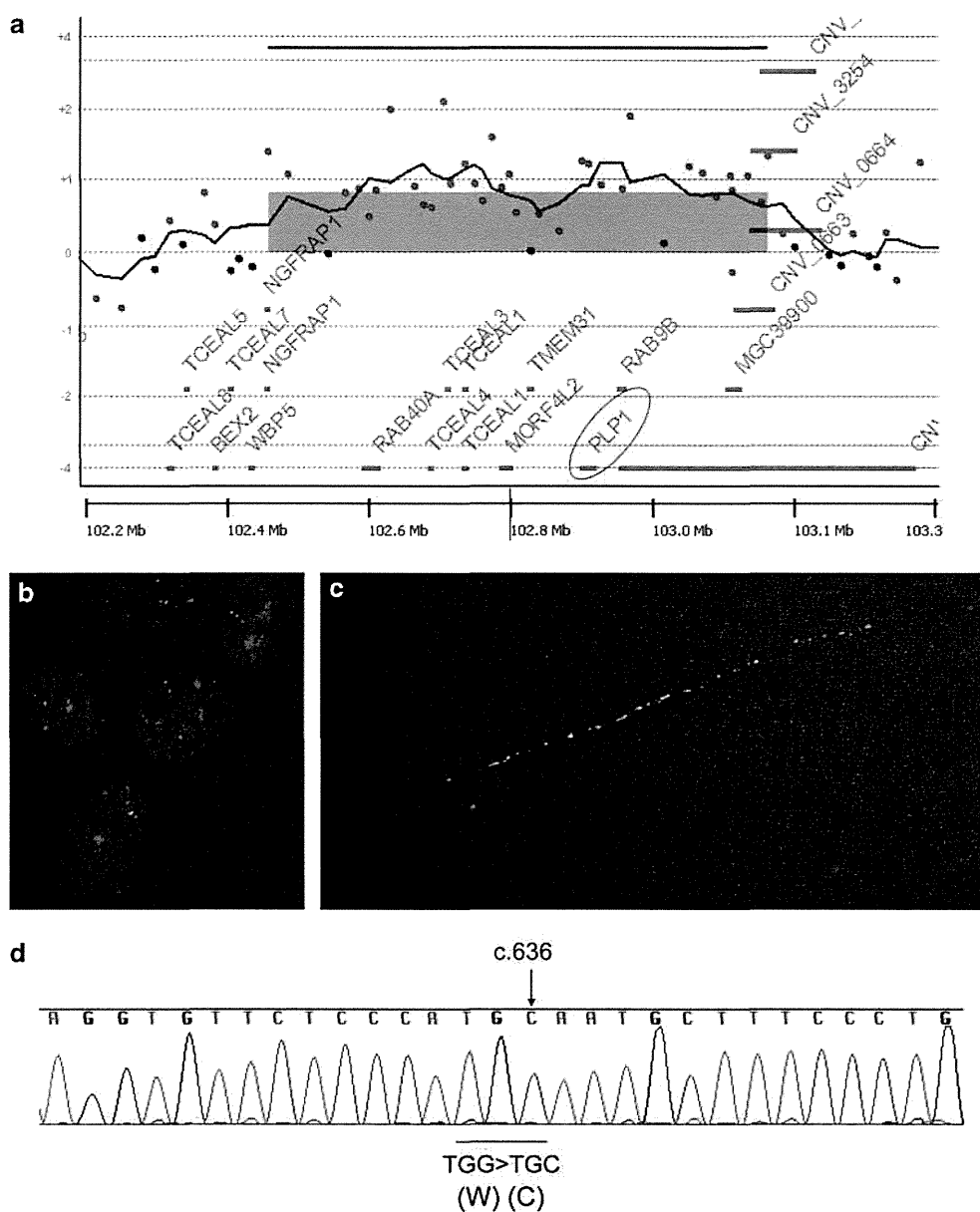


**Figure 2** Genotyping and cytogenetic analyses for Patients 2 and 3. (a) A microchromosomal duplication including *PLP1* is shown in GeneView of Agilent Genomic Workbench (Agilent Technologies). The location of *PLP1* is highlighted by a red circle. (b) Interphase fluorescence *in-situ* hybridization analysis shows two green signals labeled on RP11-832L2 (located at Xq22.2) in the nucleus. Red signals labeled on RP11-75D20 (located at Xp22.13) are the marker for X chromosome. (c) Fiber-fluorescence *in-situ* hybridization analysis indicates tandem configuration of the duplicated segments labeled with green and red probes. (d) Electropherogram shows a novel missense mutation c.636G>C (W212C) in Patient 3.

### Generation of iPS cells

We successfully generated iPS cells from three patients with PMD and a normal male control (Supplementary Figure 1). At least three independent clones were validated using the following three categories: (1) silencing of four transfected genes (*OCT3/4*, *C-MYC*, *KLF4* and *SOX2*; Supplementary Figure 2); (2) expression of endogenous pluripotency genes (*OCT3/4*, *SOX2*, *KLF4*, *C-MYC*, *NANOG* and *REX1*; Supplementary Figures 3 and 5); and (3) confirmation of the differentiation potency by immunocytochemistry (Supplementary Figure 4). Karyotype and aCGH analyses for the resulting iPS cells showed no artificial chromosomal rearrangements.

### PLP1 expression

Preliminary *PLP1* expression levels were compared between two online data sets for human skin fibroblasts and iPS cells. The results showed that *PLP1* expression levels were  $\times 40.70$  ( $\log_2 = 6.38$ ) higher in iPS cells than in skin fibroblasts (Supplementary Figure 6). Subsequently, our initial experiments for *PLP1* expression in several samples were performed by northern blot analysis, which revealed predominant *PLP1* expression in the brain (fetal brain had weaker expression than adult brain). Although the other samples showed no *PLP1* expression, we could detect the *PLP1* band in iPS cells (Figure 4); the differentiation between two isoforms for *PLP1* and *DM20* could not be detected owing to small size differences as same as